

Comparison and correlation of structural disorder caused by anion Frenkel in affecting ion conduction of $\text{La}_2\text{Hf}_2\text{O}_7$ and $\text{La}_2\text{Mo}_2\text{O}_9$ as high performance electrolyte in SOFC

Mingzi Sun and Bolong Huang*

Department of Applied Biology and Chemical Technology, The Hong Kong Polytechnic University, Hung Hom, Kowloon, Hong Kong SAR, China

*Email: bhuang@polyu.edu.hk

Abstract

$\text{La}_2\text{Hf}_2\text{O}_7$ and $\text{La}_2\text{Mo}_2\text{O}_9$ as potential electrolytes for solid oxide fuel cells (SOFCs) have been investigated through first-principles calculations to understand the mechanism of ion motion. In $\text{La}_2\text{Hf}_2\text{O}_7$, three unique types of positions that can form anion-Frenkel (a-Fr) pair have been screened out and a reasonable continuous diffusion path constructed by these migration sites has also been suggested to be the cause of ion conduction. Excellent ion conductivity in $\text{La}_2\text{Mo}_2\text{O}_9$ is more based on the short range disordered in loose and mobile structure. The thermodynamic properties of $\text{La}_2\text{Mo}_2\text{O}_9$ than $\text{La}_2\text{Hf}_2\text{O}_7$ shows that the formation of a-Fr in $\text{La}_2\text{Mo}_2\text{O}_9$ starts at lower temperature because of the higher degree of structural disorder with less constraints on oxygen ions.

Introduction

Due to the limited fossil resources have been quickly consumed, intensive research has been concentrated on renewable green energy, in which SOFCs^[1-4] have become the most important one based on their high-energy conversion efficiency and environment benignity. However, their main drawback high working temperature (800~1000 °C) not only constrains the electrolytes and electrodes but also cause unexpected products at interfaces. To develop more potential electrolyte material that improve the performance of SOFCs and lower the working temperature, we should understand the mechanism between lattice structure and ion mobility, which determines the ion conductivity of materials. As potential electrolyte material with good ion conductivity, the complexity between ion conductivities and intrinsic defects in the pyrochlore host structure has been discussed a lot with^[5-9] and their ion conductivity are usually attributed to the migration of oxygen anions caused by lattice distortion with assistance from formation of defects. In previous study, a-Fr pairs of O ion in other different lattice system all shows low formation energy^[8, 10, 11], which might be the initiation of ion conduction. The less restrictive structure with incorporative environment for interstitial migration ions will associate with better ion conduction. Recently, lanthanoid hafnates ($\text{Ln}_2\text{Hf}_2\text{O}_7$) with good ion conductivity and thermal stability have been attracted a lot interest for various applications^[12-16] based on their unique pyrochlore structures deviated from the fluorite phase with distortions^[17, 18]. Another new fast ion conductor $\text{La}_2\text{Mo}_2\text{O}_9$ ^[19, 20], showing competitive ion conductivity with present electrolyte, also attract much interest due to their relative loose structure with highly mobile oxygen ions is believed to be the main reason of their excellent ion conductivity. Similarly, these two types of materials both share great tolerance of structure and the mobility of anion ions in structure, which inspire us to investigate the correlation between defective structure and ion conduction. Here, through density function theory (DFT) as a powerful tool^[21-24], we will investigate the energetic and electronic properties of $\text{La}_2\text{Hf}_2\text{O}_7$ and $\text{La}_2\text{Mo}_2\text{O}_9$ in terms of the formation process

of a-Fr pairs, correlation between the local structure and energetics, electronic properties. The thermodynamics properties will also be discussed because it represents the formation temperature of defects that are the motivation of ion mobility, which will further result in ion conduction. By understanding the migration mechanism of oxygen anions diffusion, we can apply this effective method to further screen novel materials for future SOFCs to satisfy higher requirements with better electrical performance.

Calculation Setup

All the calculations choose the total energy density functional pseudopotential method. The Broyden-Fletcher-Goldfarb-Shannon (BFGS) algorithm will be used through calculations. For bulk properties and defect, ultrafine quality with a plane-wave cutoff energy of 750 eV and a $2 \times 2 \times 2$ Monkhost-Pack (MP) k-point mesh are used, which converged the total energy within 5.0×10^{-6} and 5.0×10^{-5} eV/atom, respectively. Crystal Structures of both ion conductors are shown in Figure S1 and S2 in Supplementary material.

Results and Discussion

Anion Frenkel Pair Defect in $\text{La}_2\text{Hf}_2\text{O}_7$

The oxygen vacancy (V_O) and the interstitial (I_O) pair are called a-Fr pair. Oxygen atoms at 48f sites with more mobility will be chosen to form a-Fr pair and the energy simulation results a-Fr pairs can be classified into three characteristic types of migration sites with corresponding average formation energy shown in Table 1 and Figure 1. The formation energies of oxygen interstitial defects are also listed for comparison.

Table 1. The average formation energies (eV/pair) of a-Fr and I_O in $\text{La}_2\text{Hf}_2\text{O}_7$.

Disorder	A-Fr formation energy (eV/pair)	A-Fr formation energy (eV/site)	I_O defect formation energy (eV/site)
TYPE 1	3.49	1.75	5.81
TYPE 2	6.53	3.27	6.12
TYPE 3	8.45	4.23	6.27

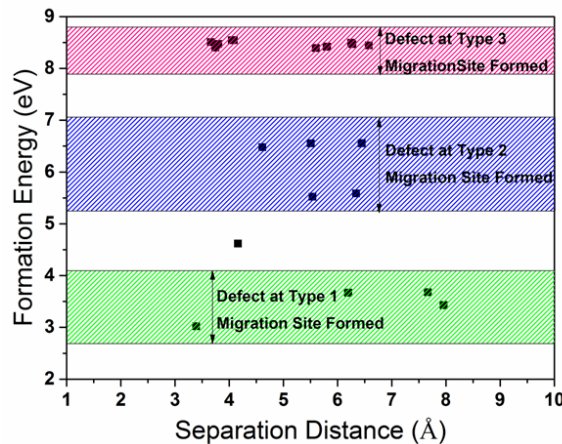


Figure 1. The diagram of formation energies (per pair) of a-Fr pairs with reference of separation (in angstrom) of the a-Fr pairs in pyrochlore $\text{La}_2\text{Hf}_2\text{O}_7$ system.

The vacant 8a sites, showing lowest energy cost of 3.49eV, are found to be the most reasonable migration site to incorporate interstitial oxygen atom to form a-Fr pairs (shown in Figure 2a)

without inducing distortion on adjacent atoms. The second type of site is a 3-fold site (shown in Figure 2b) that is discovered near the face of the La-tetrahedral with higher formation energy of 6.53 eV/pair that come along with three equivalently long La-O bonds. Type 3 migration sites is near 48f site and display the highest energy of 8.45 eV that induced by the strong O=O bond, where a plane quadrangle will be formed with 2 oxygen atoms and 2 La atoms (shown in Figure 2c) and cause obvious distortion on nearby oxygen atom. Each type of defect site show similar energy results based on different migration distances. The TDOS of all these three types of defect all reflected gap states as deep localized hole levels induced by formation of a-Fr pairs (shown in Figure S3).

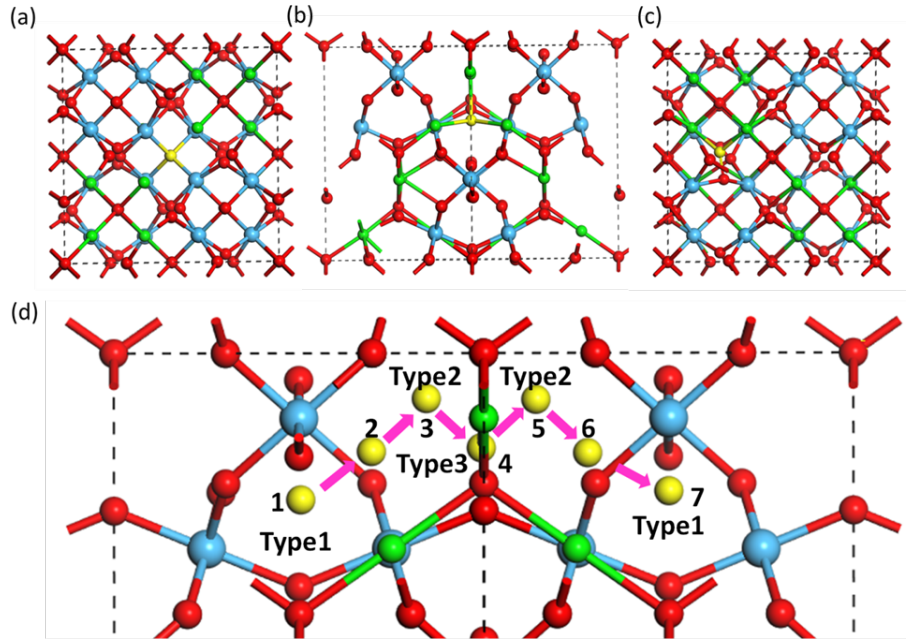


Figure 2. The relaxed structure of three a-Fr pairs in $\text{La}_2\text{Hf}_2\text{O}_7$ and proposed migration path for O ions migration. (a) Type 1 migration site (b) Type 2 migration site. (c) Type 3 migration site. (d) Diagram of proposed migration path for oxygen anions between vacant 8a sites. The pink arrows show the migration direction of oxygen anions. The yellow atom represents the interstitial oxygen atom at each type of migration sites. (La=green, Hf=blue, and O=red)

The position of each site shows correlations through constructing a continuous diffusion channels for interstitial oxygen atoms to migrating through lattice (Figure 2d), which clearly represented a path of oxygen atoms between Type1 (8a site) sites. The complete diffusion process can be concluded as: 48f (origin) \rightarrow Type 1 \rightarrow Type 2 \rightarrow Type 3 \rightarrow Type 2 \rightarrow Type 1. In contrast with a-Fr pairs, simulation results of interstitial oxygen defect show much higher energy cost in formation process without obvious energy difference levels at the same type of migration sites (shown in Table 1). This means a straitened circumstance that oxygen atoms will be easier to be trapped in one position rather than keep migrating in the lattice. Hence, the a-Fr pairs show substantial priority in pyrochlore structure than the interstitial oxygen defect. The ion motion in pyrochlore-type $\text{La}_2\text{Hf}_2\text{O}_7$ can be attributed to the structural disorder and migration path supplied by a-Fr pairs.

Anion Frenkel in La₂Mo₂O₉

La₂Mo₂O₉ has a relative loose crystal structure with low symmetry that is similar with a polyhedron-like cage (Figure S2a). The average coordination number for La and Mo atom are 6.5 and 4.50, respectively. Three non-equivalent oxygen positions exist in the structure, O1, O2 and O3 with partial occupancy. The preliminary geometry optimization of flawless unit cell reflects high mobility of O atoms with larger moving distance than metal atoms. Results of a-Fr pairs models illustrate the change of bonding along with the varied coordination number of cation atoms in Table 2. Though past researches focused more on the effects of Mo atoms as key factor in the whole system rather than La atoms^[25, 26] does, coordination number of La has shown larger variation range than Mo, representing higher distortion of local environment. The coordination number of La has shown a linear relationship with the formation energy of La₂Mo₂O₉ in certain degree (Figure S3). As the formation energy increases, the coordination number of La has a trend of gradually decreasing, reflecting that La can stabilize the structure by forming La-O bonds. The energy difference between these models can reach up to 1.79 eV with same number of divalent O=O bond, suggesting these bonds are not effective in influencing the formation of a-Fr pairs.

Table 2. The calculated average formation energies (eV/pair) and coordinated number of atoms of different anion defect in La₂Mo₂O₉.

Model	No. Of O=O bonds	Coordination No. Of La	Coordination No. Of Mo	Formation Energy (eV)
Unit cell	/	6.50	4.50	/
1	1	6.75	4.50	0.182
2	1	6.75	4.75	0.407
3	1	6.00	4.50	0.622
4	1	6.50	4.50	0.630
5	1	6.00	4.75	1.241
6	1	6.75	4.75	1.332
7	1	6.25	4.75	1.970
8	0	7.75	4.75	-5.703

Comparing with La₂Hf₂O₇, La₂Mo₂O₉ structure is more complicated with intrinsic oxygen vacancies. The potential sites in La₂Mo₂O₉ could incorporate a-Fr pairs shows lower energy cost but without obvious regulation due to the low symmetrical lattice. We speculate that the ion conductivity of La₂Mo₂O₉ is induced by the original lattice with low constraints on oxygen atoms with the assistance of a-Fr pairs. A-Fr pairs in La₂Hf₂O₇ affect the energy barriers for ion diffusion through forming a continuous migration path with distinct energy levels while the short-range hopping mechanism of oxygen ions in between present oxygen atom positions and intrinsic oxygen vacancies might be the main cause of ion conduction La₂Mo₂O₉.

Thermodynamic properties

We now consider the thermodynamic properties for these two systems based on equation: $\Delta G = \Delta E + \Delta ZPE - T\Delta S$, where ΔE is the total energy change for the defect formation, ΔZPE is the change in zero-point energies of the system compared to the ideal structure. Figure 3a shows the ΔG for the ideal system without a defect and the zero-point energies of these two systems are 2.25 eV and 1.35 eV respectively for La₂Hf₂O₇ and La₂Mo₂O₉. Figure 3b shows the effect from

difference of oxygen occupancy in $\text{La}_2\text{Mo}_2\text{O}_9$. Model 4_10 shows higher occupancy rate for the O2 and O3 with the higher level of ZPE. It tells in physicochemical trend that the degree of the structural disordering determines the ZPE of the SOFC host system, and the higher symmetry the higher ZPE. We further summarized the concept of ΔG with formation process of a-Fr pairs. In Figure 3c and 3d, we divide the temperature into three stages, preparation, trapping and conducting respectively. As temperature increases, the lattice vibration increases at the preparation stages. The start of trapping stages represents the spontaneous formation of a-Fr pairs. As the concentration of a-Fr increases with temperature, the ion motion become more active and ion conduction will start, which can be considered as the working temperature. $\text{La}_2\text{Mo}_2\text{O}_9$ shows a working temperature lower than 700 K while $\text{La}_2\text{Hf}_2\text{O}_7$ is around 750 K, indicating the structural disorder can possibly decrease the working temperature and increase the density of O-ion related transporting defect concentrations in way of forming a-Fr pairs, but the energy barrier for activating them from the trapping to conducting stage are both around 450 K.

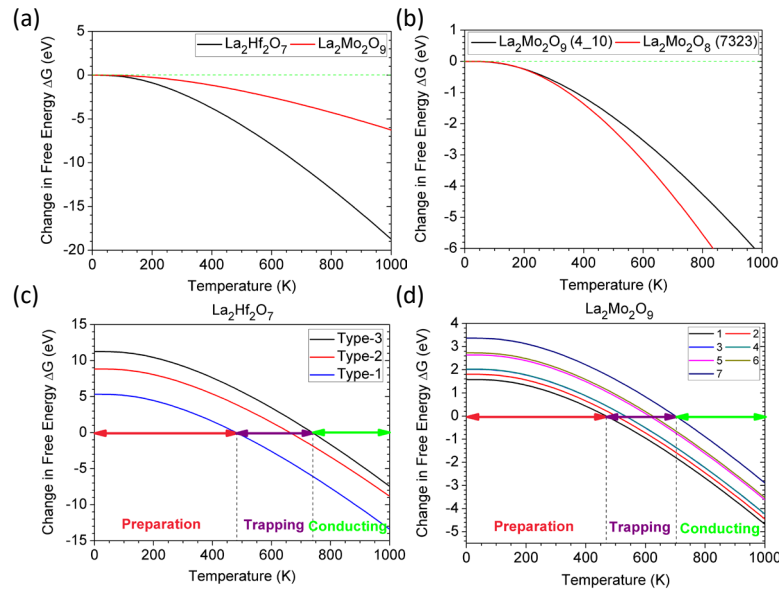


Figure 3. (a) The summary of ΔG between pyrochlore $\text{La}_2\text{Hf}_2\text{O}_7$ and $\text{La}_2\text{Mo}_2\text{O}_9$. (b) The summary of the ΔG between two different La-Mo-O systems. (c) The ΔG with consideration of the a-Fr pairs in $\text{La}_2\text{Hf}_2\text{O}_7$ system. (d) The ΔG with consideration of the a-Fr pairs in $\text{La}_2\text{Mo}_2\text{O}_9$ system.

Conclusion

This work showed a detailed study of the relationship between structural disorder of $\text{La}_2\text{Hf}_2\text{O}_7$ and $\text{La}_2\text{Mo}_2\text{O}_9$ and their ion conduction behaviors. A continuous diffusion path for interstitial O composed by three unique migration sites caused by a-Fr pairs is found to be the dominant source of ion conductivity in $\text{La}_2\text{Hf}_2\text{O}_7$. The results of $\text{La}_2\text{Mo}_2\text{O}_9$ show less regulation and their ion conductivity can be attributed to the naturally dynamic structural frame with short-range disorder and high concentration of mobile oxygen atoms. In addition, the thermodynamics calculations prove that higher degree of structural disorder in $\text{La}_2\text{Mo}_2\text{O}_9$ than $\text{La}_2\text{Hf}_2\text{O}_7$ can lower the working temperature of ion conduction. Understanding the correlation between lattice defective structure and their ion conduction will benefit us in the future to screen out more possible electrolyte materials and predicting their electrical performance in SOFCs.

Acknowledgement

The author BH gratefully acknowledges the support of the Natural Science Foundation of China (NSFC) for the Youth Scientist grant (Grant No.: NSFC 11504309), the initial start-up grant support from the Department General Research Fund (Dept. GRF) from ABCT in the Hong Kong Polytechnic University (PolyU), and the Early Career Scheme (ECS) fund (Grant No.: PolyU 253026/16P) from the Research Grant Council (RGC) in Hong Kong. This work is supported by the high performance supercomputer (ATOM-project) in Dept. of ABCT of PolyU.

References

1. N. Minh, *Solid State Ionics* **1-4**(174), 271-277.(2004).
2. S. Singhal, *Solid State Ionics* **1-4**(135), 305-313.(2000).
3. A. B. Stambouli and E. Traversa, *Renewable and Sustainable Energy Reviews* **5**(6), 433-455.(2002).
4. N. Q. Minh, *J. Am. Ceram. Soc.* **3**(76), 563-588.(1993).
5. A. Burggraaf, T. Vandijk and M. Verkerk, *Solid State Ionics* **5**, 519-522.(1981).
6. M. Vandijk, A. Burggraaf, A. Cormack and C. Catlow, *Solid State Ionics* **2**(17), 159-167.(1985).
7. W. P. and C. C.R.A., *Solid State Ionics* **3-4**(112), 173-183.(1998).
8. L. Minervini, R. W. Grimes and K. E. Sickafus, *J. Am. Ceram. Soc.* **8**(83), 1873-1878.(2004).
9. T. Hagiwara, H. Yamamura and H. Nishino, *IOP Conference Series: Materials Science and Engineering* **13**(18), 132003.(2011).
10. B. Huang, R. Gillen and J. Robertson, *The Journal of Physical Chemistry C* **42**(118), 24248-24256.(2014).
11. P. Wilde and C. Catlow, *Solid State Ionics* **3-4**(112), 173-183.(1998).
12. H. Lehmann, D. Pitzer, G. Pracht, R. Vassen and D. Stöver, *J. Am. Ceram. Soc.* **8**(86), 1338-1344.(2003).
13. Y. Eagleman, M. Weber, A. Chaudhry and S. Derenzo, *J. Lumin.* **11**(132), 2889-2896.(2012).
14. Y. Ji, D. Jiang and J. Shi, *J. Mater. Res.* **03**(20), 567-570.(2011).
15. G. R. Lumpkin, K. R. Whittle, S. Rios, K. L. Smith and N. J. Zaluzec, *J. Phys.: Condens. Matter* **47**(16), 8557-8570.(2004).
16. R. C. Ewing, W. J. Weber and J. Lian, *J. Appl. Phys.* **11**(95), 5949-5971.(2004).
17. H. Yamamura, *Solid State Ionics* **3-4**(158), 359-365.(2003).
18. E. Aleshin and R. Roy, *J. Am. Ceram. Soc.* **1**(45), 18-25.(1962).
19. P. Lacorre, F. Goutenoire, O. Bohnke, R. Retoux and Y. Laligant, *Nature* **6780**(404), 856-858.(2000).
20. F. Goutenoire, O. Isnard and R. Retoux, *Chem. Mater.* **9**(12), 2575-2580.(2000).
21. R. Terki, H. Feraoun, G. Bertrand and H. Aourag, *J. Appl. Phys.* **11**(96), 6482-6487.(2004).
22. J. M. Pruneda and E. Artacho, *Physical Review B* **8**(72), 2005).
23. N. Li, H. Y. Xiao, X. T. Zu, L. M. Wang, R. C. Ewing, J. Lian and F. Gao, *J. Appl. Phys.* **6**(102), 063704.(2007).
24. W. R. Panero, L. Stixrude and R. C. Ewing, *Physical Review B* **5**(70), 2004).
25. I. R. Evans, J. A. K. Howard and J. S. O. Evans, *Chem. Mater.* **16**(17), 4074-4077.(2005).
26. P. Lacorre, A. Selmi, G. Corbel and B. Boulard, *Inorg. Chem.* **2**(45), 627-635.(2006).